SIMULATION OF THE GRAVITATIONAL COLLAPSE AND FRAGMENTATION OF ROTATING MOLECULAR CLOUDS

P. Berczik[1,2], **M. I. Petrov**[1]

[1] *Main Astronomical Observatory, NAS of Ukraine*
27 Akademika Zabolotnoho Str., 03680 Kyiv, Ukraine
e-mail: berczik@mao.kiev.ua; petrov@mao.kiev.ua

[2] *Astrophysics Group, Department of Physics, Rochester Institute of Technology*
54 Lomb Memorial Drive, Rochester, NY 14623, USA
e-mail: berczik@cis.rit.edu

In this paper we study the process of the subsequent (runaway) fragmentation of a rotating isothermal Giant Molecular Cloud (GMC) complex. Our own Smoothed Particle Hydrodynamics (SPH) gas-dynamical model successfully reproduces the observed Cloud Mass-distribution Function (CMF) in our Galaxy (even the differences between the inner and outer parts of our Galaxy). The steady state of CMF is established during the collapse within a free-fall timescale of the GMC. We show that one of the key parameters, which defines the observed slope of the present day CMF, is the initial ratio of the rotational (turbulent) and gravitational energy inside the fragmented GMC.

INTRODUCTION

The SPH algorithm based on 3D hydrodynamical codes, starting with the series of pioneering works by Monaghan and Lattanzio [8, 13, 14, 17], are always very successfully applied to the study of evolution and fragmentation in molecular clouds and molecular cloud complexes. The early simulations have been usually performed with a few hundred to a few thousand of SPH particles and with a fixed (few parsec) spatial resolution. The most up-to-date simulations of molecular cloud evolution (*e.g.*, [15]) are performed using a few tens of thousands of SPH particles with variable smoothing lengths. These simulations also include the details of cooling and heating in the complex gas mixtures of H, H_2, CO and H II species.

Our high-resolution (64 000 SPH particle) simulations, using highly flexible and adaptive smoothing lengths, deal with the study of the runaway collapse and subsequent isothermal fragmentation of an isolated GMC complex with different rotational (turbulent) energy parameters of the clouds. The resulting CMF is compared with the recent observational distributions of molecular cloud complexes ($dN/dM \sim M^{-\gamma}$, where the slope of the power law γ ranges from 1.4 to 1.8) derived from various CO data for different parts of our Galaxy [6, 10, 12, 16, 21, 22].

METHOD

Continuous hydrodynamic fields in SPH are described by the interpolation functions constructed from the known values of these functions at randomly positioned N "smooth" particles with individual masses m_i [18]. To achieve the same level of accuracy for all points in the fluid it is necessary to use a spatially variable smoothing length. In this case each particle has an individual value of the smoothing length – h_i.

A more detailed and complete description of the basic numerical equations of SPH can be found in many of our previous publications (*e.g.*, [1–4, 24] and the references herein). Therefore, we briefly repeat here the skeleton SPH equations of the code. The density at the position of a particle i can be defined as:

$$\rho_i \;=\; \sum_{j=1}^{N} m_j \cdot W_{ij},$$

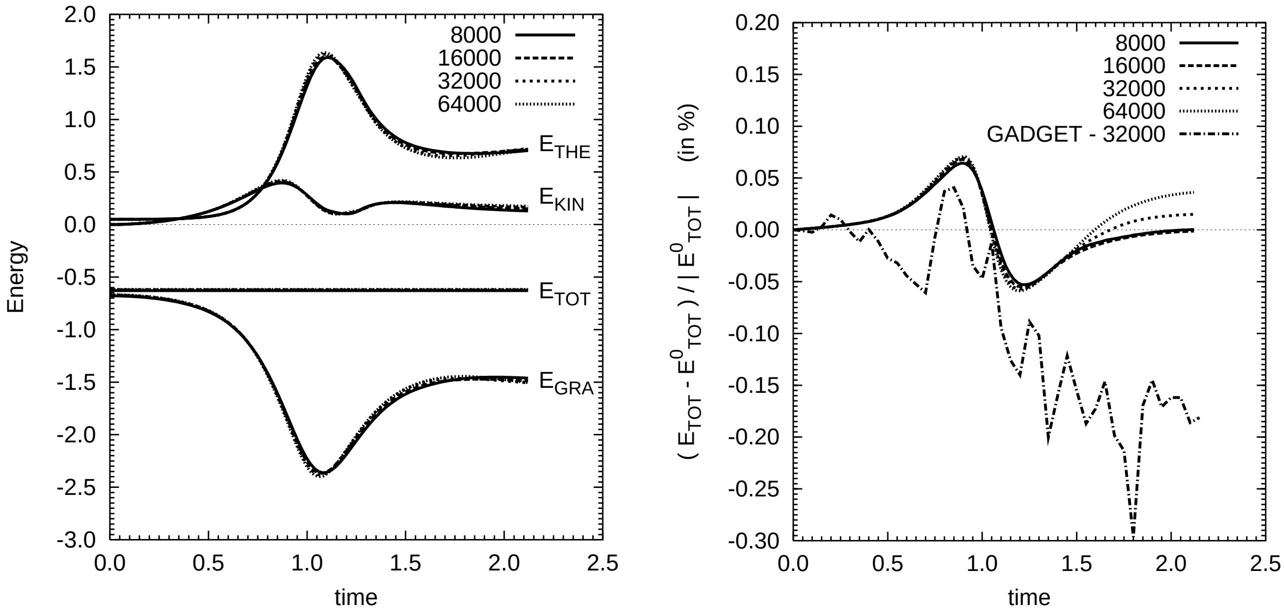

a) Evolution of the energy

b) Relative total energy error

Figure 1. Time evolution of the thermal, kinetic, potential, and total energy for the adiabatic collapse of an initially "cold" gas sphere. The different lines correspond to the different gas particle numbers. We also present the energy error results of the `GADGET` code with "standard" parameters for 32 000 particles

The equations of motion for a particle i are expressed as:

$$\frac{d\mathbf{r}_i}{dt} \;=\; \mathbf{v}_i,$$

$$\frac{d\mathbf{v}_i}{dt} \;=\; -\; \sum_{j\,=\,1}^{N} m_j \left(\frac{P_i}{\rho_i^2} \;+\; \frac{P_j}{\rho_j^2} \;+\; \tilde{\Pi}_{ij} \right) \;\nabla_i\, W_{ij} \;-\nabla_i\, \Phi_i,$$

where P_i is the pressure, Φ_i is the self-gravitational potential, and $\tilde{\Pi}_{ij}$ is an artificial viscosity term.

The internal energy equation has the form:

$$\frac{du_i}{dt} \;=\; \frac{1}{2} \sum_{j\,=\,1}^{N} m_j \; \left(\frac{P_i}{\rho_i^2} + \frac{P_j}{\rho_j^2} \;+\; \tilde{\Pi}_{ij} \right) \; (\mathbf{v}_i - \mathbf{v}_j)\; \nabla_i\, W_{ij} \;+\; \frac{\Gamma_i \;-\; \Lambda_i}{\rho_i}.$$

Here u_i is the specific internal energy of the particle i. The term $(\Gamma_i - \Lambda_i)/\rho_i$ accounts for non-adiabatic processes not associated with the artificial viscosity. We present the radiative cooling in the form proposed in [19] (see case "B"), using the `MAPPINGS III` software [26]:

$$\Lambda \;=\; \Lambda(\rho,\; u,\; Z,\; \ldots) \;\simeq\; \Lambda^*(T,\; [\mathrm{Fe/H}]) \cdot n_i^2, \qquad\qquad n_i \;=\; \rho_i/(\mu \cdot m_p),$$

where n_i is the hydrogen number density, T_i the temperature, and μ is the molecular weight.

The equation of state must be added to close the system:

$$P_i \;=\; (\gamma - 1)\; \rho_i \cdot u_i,$$

where γ is the adiabatic index.

One of the basic tasks in SPH is to find the nearest neighbours of each SPH particle, *i.e.*, to construct an interaction list for each particle. Basically, we need to find all particles with $|\;\mathbf{r}_{ij}\;| \leq 2\max(h_i,\; h_j)$ in order to estimate the density and also calculate the hydrodynamical forces.

In our code we keep the number of neighbours exactly constant by defining $2h_i$ to be the distance to the N_B – nearest particle. The value of N_B is chosen such that a certain fraction of the total number of "gas" particles N affects the local flow characteristics. From these we need to `SELECT` the closest N_B particles. Fast algorithms

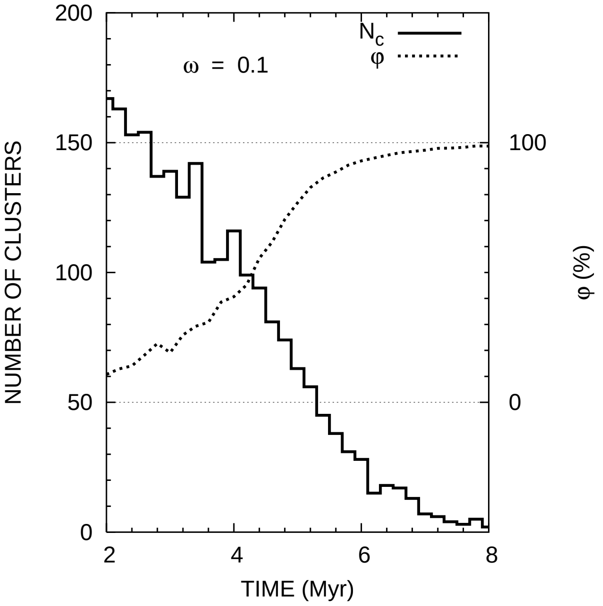

a) "Slow" initial rotation $\omega = 0.1$

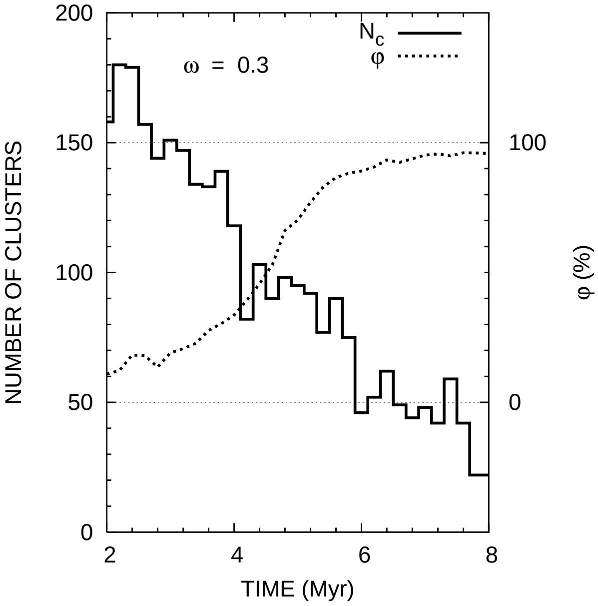

b) "Fast" initial rotation $\omega = 0.3$

Figure 2. The time evolution of the total number of clusters N_c and the total mass fraction inside these clusters ϕ during the simulations. Starting from the $\sim$ 5 Myr more than 80% of the total mass is already concentrated inside the fragments. At around 6 Myr almost 95% of the total mass is already inside the clusters

for doing this exist [20]. For computational reasons, if the defined h_i becomes smaller than the selected minimal smoothing length h_{min}, we set the value $h_i = h_{min}$.

In order to calculate the self-gravitational potential Φ_i and self-gravitational force $-\nabla_i\Phi_i$ we use the Mitaka Underground Vineyard (MUV) `GRAPE6` computer system at the National Astronomical Observatory of Japan [`http://www.cc.nao.ac.jp/muv/`]. For a more detailed description of the `GRAPE6` board and for links to publication about the `GRAPE6`, we refer the reader to the official homepage of Jun Makino at the Tokyo University [`http://grape.astron.s.u-tokyo.ac.jp/~makino/grape6.html`].

For the time integration of the system of hydrodynamical equations we use the second-order Runge–Kutta–Fehlberg scheme. The time step Δt_i for each particle depends on the particle's acceleration $\mathbf{a}_i$ and velocity $\mathbf{v}_i$, as well as on the sound speed c_i and the heating *vs.* cooling balance:

$$\Delta t \;=\; C_n \cdot \min_i \left[\sqrt{\frac{2h_i}{\mid \mathbf{a}_i \mid}}; \;\; \frac{h_i}{\mid \mathbf{v}_i \mid}; \;\; \frac{h_i}{c_i}; \;\; \frac{u_i}{\dot{u}_i} \right],$$

where C_n is the Courant's number and is equal to 0.1. For computational reasons we fix the minimal integration time step Δt_{min}.

The main aim of our current research is a detailed study of the isothermal fragmentation processes inside a collapsing "cold" molecular cloud complex. For the purpose to find the fragments and its physical parameters (mass and size), we use our own "cluster finding" algorithms. In these algorithms we modify the well known and "standard" friend-of-friend (FOF) method [11]. In addition to the use of the particle positions in the process of "constructing" or finding the clusters (fragments) we also involve the information on the density distribution inside each potential cluster. On the basis of the density distribution analysis we can finally select in the more accurate way the members of our fragments (clusters). In this sense our method is more close to the so-called `SKID` method, which is well described at the homepage of the Washington University "N-body Shop" [`http://www-hpcc.astro.washington.edu/tools/skid.html`]. Here the reader can find a more detailed description of this density basic method which is specially designed to find the gravitationally bound groups of particles in the N-body like simulations.

One of the features of our cluster finding routine is the setting of the minimum limit of gaseous particles to 5, in order to form a fragment. In other words, we do not count as "real" a cluster where the number of particles is less than 5.

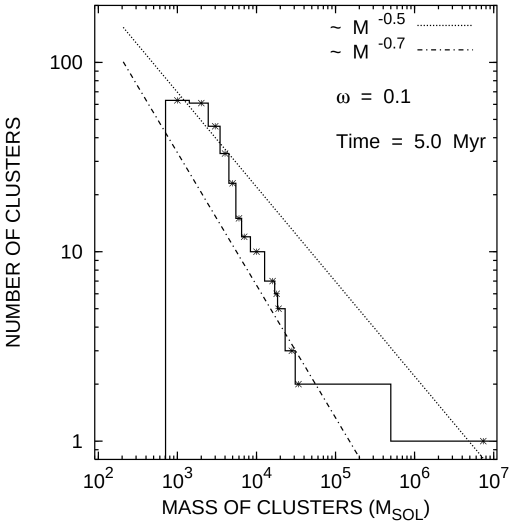

a) “Slow” initial rotation $\omega = 0.1$, time = 5 Myr

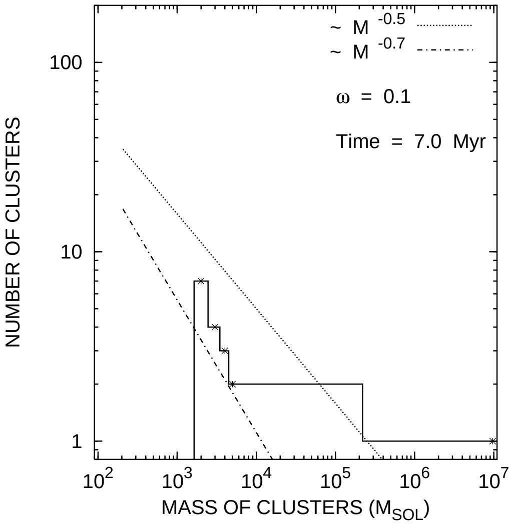

b) “Slow” initial rotation $\omega = 0.1$, time = 7 Myr

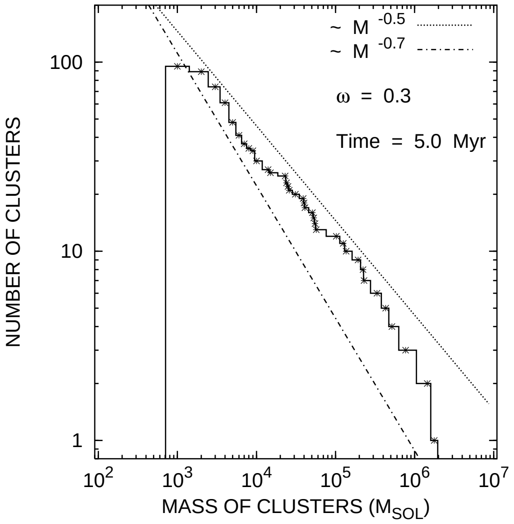

c) “Fast” initial rotation $\omega = 0.3$, time = 5 Myr

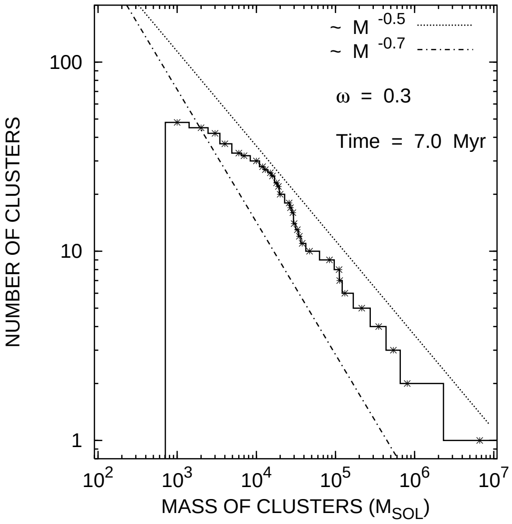

d) “Fast” initial rotation $\omega = 0.3$, time = 7 Myr

Figure 3. Four snapshots of the integrated cluster distribution function (ICMF)

CODE TESTING

The self-gravitating collapse of an initially isothermal “cold” gas sphere has been a common test problem for different SPH codes [5, 7, 9, 23, 25, 27]. Following these authors, for the testing of our code, we calculate the adiabatic evolution of the spherically symmetric gas cloud of total mass M and radius R. For the initial internal energy per unit mass we set $u = 0.05 \dfrac{GM}{R}$. The initial density profile of the cloud we obtain from

$$\rho(r) = \frac{M}{2\,\pi\,R^2}\,\frac{1}{r}.$$

We distribute randomly the gas particles inside a set of spherical shells in a manner that reproduces the initial density profile. At the start of the simulation the gas particles are at rest. For the presentation of the results we use a system of units where $G = M = R = 1$.

In Fig. 1 we show the time evolution of a different types of energy and the relative total energy errors during the calculation. For comparison of our test results we also plot the energy error results from the serial variant of the `GADGET` public access SPH-TREE code [23] with “standard” parameters for the 32 000 particles [`http://www.mpa-garching.mpg.de/gadget/`].

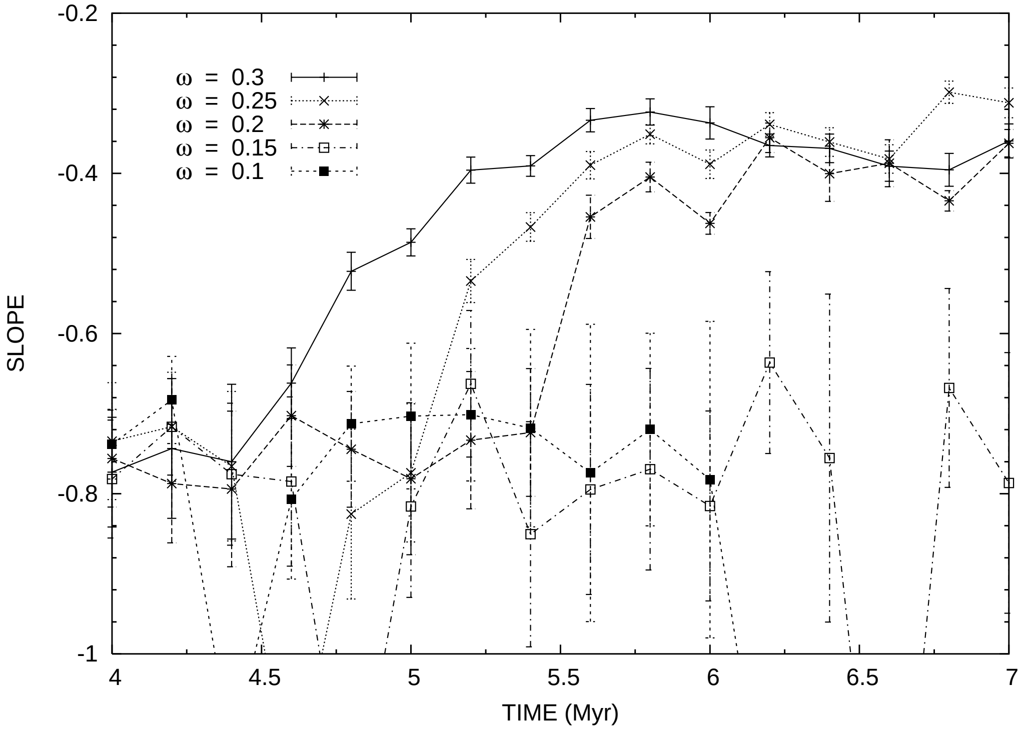

Figure 4. The ICMF slope time evolution for our models with different rotation parameters

During the central bounce around $t \approx 1.1$ most of the kinetic energy is converted into heat, and a strong shock wave travels outward. For all of these runs the number of neighbours N_B is assumed to be 50 and the gravitational softening ε is assumed to be 0.01. For the integration of the system of equations we use the second-order Runge–Kutta–Fehlberg scheme with a fixed time step $\Delta t = 10^{-4}$.

The results presented in Fig. 1 agree very well with those of [23] and [25]. The maximum relative total energy error is of around 0.05% even for moderate (8 000) particle numbers. The largest adiabatic test calculation (with 64 000 gas particles up to $t \approx 2.2$) on an Intel Pentium 4 (3.4 GHz) host machine with the `GRAPE6` board took ≈ 3.67 days of total CPU time.

INITIAL CONDITIONS

As an initial condition for our molecular cloud fragmentation study we use a model in which the parameters are comparable with the largest GMC complexes in our Galaxy [6, 10, 16]. For the mass of the system we set $M_{cloud} = 10^7\, M_\odot$. For the radius of the cloud we set $R_{cloud} = 100$ pc. For an initial density distribution we use the previous formula where $\rho(r) \sim 1/r$. For the purpose of checking the possible "resolution" effects we carry out two sets of runs with 32 000 and 64 000 gas particles (with the corresponding indexes "low" and "high"). The total gravitational energy of the system in such a case can be easily calculated using the simple formula:

$$E^0_{\rm GRA} = -\frac{2}{3}\, G\, M^2_{cloud}/R_{cloud}.$$

For the initial temperature we set the value, which produced the overall ratio of the thermal energy to the gravitational energy of the system, at the fixed level: $\alpha \equiv E^0_{\rm THE}/\,|E^0_{\rm GRA}| = 0.075$. For the previous fixed mass and radius of the system this condition produced an initial temperature of the cloud $T_{cloud} \approx 2200$ K. The corresponding sound speed was $c \approx 3.8$ km/s. This is consistent with the typical measured "kinetic" temperatures for such GMC complexes [6].

With these parameters we have an initial central concentration $n_0 \approx 10^3\,{\rm cm}^{-3}$ and a free-fall time in the cloud center $\tau_{ff} \approx 1$ Myr. The central Jeans radius R_J is ≈ 10 pc and the corresponding Jeans mass M_J is equal to about $10^5\, M_\odot$. Initially, we give the whole system a rigid rotational velocity distribution with an angular velocity value Ω_{cloud} which we set to the unity of $\Omega_0 = V_0/\,R_{cloud}$, where

$$V_0 \equiv \sqrt{G\ M_{cloud}/R_{cloud}}.$$

With the above-mentioned parameters we obtain $V_0 \approx 21$ km/s.

The main rotational parameters (ω and β) for our two sets of models are listed in Table 1.

Table 1. The list of initial "rotational" parameters in our models

$\omega \equiv \Omega_{cloud}/\Omega_0$	$=$	0.05	0.10	0.15	0.20	0.25	0.30
$\beta \equiv E_{\rm KIN}/E^0_{\rm GRA}$	$\approx$	$6.2 \cdot 10^{-4}$	$2.5 \cdot 10^{-3}$	$5.6 \cdot 10^{-3}$	$1.0 \cdot 10^{-2}$	$1.5 \cdot 10^{-2}$	$2.2 \cdot 10^{-2}$

As we can see from Table 1, the initial ratio of the rotational (or kinetic) energy of the motion of the fragments (β), even in the last models with a "high" rotational parameter, does not exceed a few percents of the gravitational bounding energy of the cloud. This value is even less for the initial ratio of the system's thermal energy to the gravitational energy ($\alpha = 7.5\%$). In all models, usually after the first few Myr of evolution, these situations have changed. The ratio β is rising to an approximate value of 0.5 or even more. Its mean is when the cloud starts the process of intensive isothermal fragmentation and the whole system of fragments becomes almost fully "rotationally" supported.

RESULTS

In Fig. 2 we show the time evolution of the total number of clusters $N_{\rm c}$ and the total mass fraction inside these clusters ϕ during the simulations. Starting from ~ 5 Myr more than 80% of the total mass is already concentrated inside the fragments. At around 6 Myr almost 95% of the total mass is already inside the clusters. Figure 2a shows the results for the "slow" rotating model with $\omega = 0.1$. In Fig. 2b we show the evolution of the "fast" rotating model with $\omega = 0.3$.

In Fig. 3 we show four different snapshots of the integrated cluster distribution function (ICMF) for two selected moments of time with two different rotational parameters ω. For practical numerical reasons we use the ICMF instead of the CMF (which is also called sometimes in the literature as the Differential Cloud Mass Function – DCMF). Here is a simple definition of the ICMF:

$$\mathrm{ICMF} = \int_0^M dN/dM.$$

Basically, it shows how many clouds we have from zero mass to any fixed mass (M). Because the CMF is usually approximated with the power law $M^{-\gamma}$ in this case the ICMF can be simply derived as $\sim M^{-\gamma+1}$.

The reason for using the ICMF instead of the CMF (DCMF) is that the averaging and slope definition is mathematically better due to the integrated CMF (which is a monotone function) and because the histograms in this case do not have any "holes". Of course when we compare our results with the observed (differential) CMF slope we need to subtract one from the ICMF slope to get the corresponding CMF slope.

In Fig. 3 we can see that in most cases the ICMF slope lies between –0.5 and –0.7 (the corresponding CMF is –1.5 and –1.7). The models with slow rotation always have a significantly lower value of the slope.

The ICMF slope time evolution for the set of our models with different rotation parameters are presented in Fig. 4. The models with initial "slow" rotational parameters give the ICMF average slope a level of –0.8 (which corresponds to the CMF slope of –1.8). The "fast" rotating models give the ICMF slope a level of –0.4 (CMF slope of –1.4).

On average all models show very close values of the CMF slopes in comparison with the observed values of γ in the different parts of our Galaxy.

The slow rotation models systematically show the slope more close to the observed values in the outer part of our Galaxy [6, 10, 12] ($\gamma \approx -1.8 \pm 0.03$). In contrast, the fast model CMF slopes is more consistent with the observations from the central part of our Galaxy [16, 21, 22] $\gamma \approx -1.5 \pm 0.1$.

Of course our simulations are time and also resolution limited, but even in this case we can derive a statement about the two significantly different types of "population" in the molecular cloud distributions. The key parameter which produces the different CMF slopes is the initial rotational parameter of the forming (and subsequently fragmenting) GMC.

CONCLUSIONS

In this paper we present a study of the subsequent (runaway) fragmentation of a rotating isothermal GMC complex. Our own Smoothed Particle Hydrodynamics (SPH) gas-dynamical model `GRAPE`'s based, successfully reproduced the observed Cloud Mass-distribution Function (CMF) in our Galaxy. The steady state of CMF is quickly established during the collapse approximately on a scale of a few free-fall time in the central parts of the modelled GMC.

One of the key points in our model is that using our results we can naturally explain the source of possible differences between the observed slope on molecular clouds mass distribution function in the Galactic center and the outer regions of our Galaxy.

The basic idea is what if the GMC formed as a result of the galactic disc instability on the scale of the disc height (∼100 pc). In such a case the initial angular momentum of the forming GMC can be defined by the Coriolis force during the formation inside the differentially rotating disc. Therefore, the central GMC has a bigger β and the external GMC has a smaller rotational parameter.

According to our models this produces the different slopes of the resulting CMF during the runaway fragmentation process inside the system. The observed CMF gives to the central parts of Galaxy a slope well approximated with the value $\gamma \approx -1.5 \pm 0.1$ [16, 21, 22] and for the outer parts of the Galaxy the approximate value $\gamma \approx -1.8 \pm 0.03$ [6, 10, 12].

Our results for the "slow" and "fast" rotating models give us exactly the same slopes which have a very good agreement with the recent observations. The "slow" models corresponds to the initially more slowly rotating GMC in the outer parts of the Galaxy. The "fast" rotating models corresponds to the GMC in the central part of the Galaxy. The central GMC can initially get a greater angular momentum from the differential rotation of the galactic disc during the process of GMC formation itself.

Our numerical investigation clearly shows that one of the key parameters, which determines the observed slope of the present day molecular CMF in different parts of our Galaxy, is the initial ratio of the rotational (turbulent) and gravitational energy inside the forming GMC.

Acknowledgements. P. B. wish to express his thanks for the support of his work to the German Science Foundation (DFG) under the grant **SFB-439** (sub-project **B5**). P. B.'s work was also supported by the following grants: **NNG04GJ48G** from NASA, **AST-0420920** from NSF and by **HST-AR-09519.01-A** from STScI. He is very grateful for the hospitality to the Astronomisches Rechen-Institut (Heidelberg, Germany) where a part of this work has been done. The research work of the authors was also supported by the Ukrainian State Fund of Fundamental Investigations within the framework of the project **02.07.00132**.

The calculation has been performed with the Mitaka Underground Vineyard (MUV) `GRAPE6` system of the National Astronomical Observatory of Japan. The authors want to express their special thanks to colleague Naohito Nakasato (Computational Astrophysics Group, RIKEN) for his permanent help and support in handling of the NAOJ `GRAPE6` computational facilities.

The authors are also very grateful to Dan Batcheldor (Astrophysics Group, RIT) for his constructive comments to the first variant of the paper.

[1] *Berczik P.* Chemo – Dynamical Smoothed Particle Hydrodynamic code for evolution of star forming disk galaxies // Astron. and Astrophys.–1999.–**348**.–P. 371–380, [astro-ph/9907375].

[2] *Berczik P.* Modeling the star formation in galaxies using the Chemo – Dynamical SPH code // Astrophys. and Space Sci.–2000.–**271**.–P. 103–126, [astro-ph/0007279].

[3] *Berczik P., Hensler G., Theis Ch., Spurzem R.* Chemodynamical Modeling of Galaxy Formation and Evolution // Astrophys. and Space Sci.–2002.–**281**.–P. 297–300, [astro-ph/0112308].

[4] *Berczik P., Hensler G., Theis Ch., Spurzem R.* Multi – Phase Chemo – Dynamical SPH code for galaxy evolution // Astrophys. and Space Sci.–2003.–**284**.–P. 865–868, [astro-ph/0301531].

[5] *Carraro G., Lia C., Chiosi C.* Galaxy formation and evolution – I. The Padua TREE-SPH code (PD-SPH) // Mon. Notic. Roy. Astron. Soc.–1988.–**297**.–P. 1021–1040.

[6] *Dame T.M., Hartmann D., Thaddeus P.* The Milky Way in molecular clouds: a new complete CO survey // Astrophys. J.–2001.–**547**.–P. 792–813.

[7] *Evrard A. E.* Beyond N-body – 3D cosmological gas dynamics // Mon. Notic. Roy. Astron. Soc.–1988.–**235**.–P. 911–934.

[8] *Gingold R. A., Monaghan J. J.* On the fragmentation of differentially rotating clouds // Mon. Notic. Roy. Astron. Soc.–1983.–**204**.–P. 715–733.

[9] *Hernquist L., Katz N.* TREESPH: A unification of SPH with the hierarchical TREE method // Astrophys. J. Suppl. Ser.–1989.–**70**.–P. 419–446.

[10] *Heyer M. H., Carpenter J. M., Snell R. L.* The equilibrium state of molecular regions in the outer Galaxy // Astrophys. J.–2001.–**551**.–P. 852–866.

[11] *Huchra J. P., Geller M. J.* Groups of galaxies. I. Nearby groups // Astrophys. J.–1982.–**257**.–P. 423–437.

[12] *Kramer C., Stutzki J., Rohrig R., Corneliussen U.* Clump mass spectra of molecular clouds // Astron. and Astrophys.–1998.–**329**.–P. 249–264.

[13] *Lattanzio J. C., Henriksen R. N.* Collisions between rotating interstellar clouds // Mon. Notic. Roy. Astron. Soc.–1988.–**232**.–P. 565–614.

[14] *Lattanzio J. C., Monaghan J. J., Pongracic H., Schwarz M. P.* Interstellar cloud collisions // Mon. Notic. Roy. Astron. Soc.–1985.–**215**–P. 125–147.

[15] *Marinho E. P., Lépine J. R. D.* SPH simulations of clumps formation by dissipative collision of molecular clouds // Astron. and Astrophys. Suppl. Ser.–2000.–**142**.–P. 165–179.

[16] *Miyazaki A., Tsuboi M.* Dense molecular clouds in the Galactic center region. II. Statistical properties of the Galactic center molecular clouds // Astrophys. J.–2000.–**536**.–P. 357–367.

[17] *Monaghan J. J., Lattanzio J. C.* A simulation of the collapse and fragmentation of cooling molecular clouds // Astrophys. J.–1991.–**375**.–P. 177–189.

[18] *Monaghan J. J.* Smoothed Particle Hydrodynamics // Annu. Rev. Astron. and Astrophys.–1992.–**30**.–P. 543–574.

[19] *Nakasato N., Mori M., Nomoto K.* Numerical simulation of globular cluster formation // Astrophys. J.–2000.–**535**.–P. 776–787.

[20] *Press W. H., Teukolsky S. A., Vetterling W. T., Flannery B. P.* Numerical recipes in C.–Cambridge: Cambridge University Press, 1995.

[21] *Sanders D. B., Scoville N. Z., Solomon P. M.* Giant molecular clouds in the Galaxy. II. Characteristics of discrete features // Astrophys. J.–1985.–**289**.–P. 373–387.

[22] *Solomon P.M., Rivolo A.R., Barrett J., Yahil A.* Mass, luminosity, and line width relations of Galactic molecular clouds // Astrophys. J.–1987.–**319**.–P. 730–741.

[23] *Springel V., Yoshida N.* GADGET: a code for collisionless and gasdynamical cosmological simulations // New Astronomy.–2001.–**6**.–P. 79–117.

[24] *Spurzem R., Berczik P., Hensler G., et al.* Multi – Phase Chemo – Dynamical SPH code for galaxy evolution // Publ. Astron. Soc. Austral.–2004.–**21**.–P. 1–4, [astro-ph/0311482].

[25] *Steinmetz M., Müller E.* On the capabilities and limits of smoothed particle hydrodynamics // Astron. and Astrophys.–1993.–**268**.–P. 391–410.

[26] *Sutherland R. S., Dopita M. A.* Cooling functions for low-density astrophysical plasmas // Astrophys. J. Suppl. Ser.–1993.–**88**.–P. 253–327.

[27] *Thacker R.J., Tittley E.R., Pearce F.R., et al.* Smoothed Particle Hydrodynamics in cosmology: a comparative study of implementations // Mon. Notic. Roy. Astron. Soc.–2000.–**319**.–P. 619–648.